

Theoretical and experimental analysis of the accuracy and reproducibility of cell tracking velocimetry

M. Nakamura, M. Zborowski, L. C. Lasky, S. Margel, J. J. Chalmers

Abstract A theoretical and experimental analysis has been conducted to determine the accuracy of cell tracking velocimetry (CTV). CTV is an analytical technique for quantifying magnetically induced velocity of immunomagnetically labeled cells (or particles), in which the computer algorithm, particle tracking velocimetry (PTV), has been modified and combined with a well-defined magnetic energy gradient. In addition, this technique can calculate the size of a cell (or particle) through the use of experimentally measured settling velocities. A model was developed which determines the minimum and maximum cell velocities that can be determined based on a number of intrinsic constants and variables associated with this technique. This model was experimentally tested using a number of calibration particles and very good agreement between model and experimental data was obtained. The combination of model and experimental validation establishes the proper operating parameters for CTV.

List of symbols

B	magnetic flux density
D_p	particle diameter (mm)
F	force
g	gravity (m/s^2)
L_h	height of monitored rectangle area (mm)
L_w	width of monitored rectangle area (mm)

L_m	CTV-calculated distance of the movement of the cell in n_c frames (mm)
L_{ph}	height of 1 pixel (mm)
L_{pw}	width of 1 pixel (mm)
m	magnetophoretic mobility of a particle ($\text{mm}^3/\text{T A s}$)
n_{ph}	number of pixels in height of an image of the monitored rectangle area (pixel)
n_{pw}	number of pixels in width of an image of the monitored rectangle area (pixel)
n_c	number of frames used for a calculation of cell velocities in 2-D tracking module of CTV algorithm (frame)
t_f	time interval between successive frames (s)
u	velocity of the particle toward x direction (perpendicular to gravity direction) (mm/s)
u_{max}	maximum velocity of the particle toward x direction that CTV algorithm theoretically obtains (mm/s)
u_{min}	minimum velocity of the particle toward x direction that CTV algorithm theoretically obtains (mm/s)
v	velocity of the particle toward y direction (parallel to gravity direction) (mm/s)
v_{max}	maximum velocity of the particle toward y direction that CTV algorithm theoretically obtains (mm/s)
v_{min}	minimum velocity of the particle toward y direction that CTV algorithm theoretically obtains (mm/s)
V_p	particle volume (mm^3)

Received: 14 January 2000/Accepted: 10 July 2000

M. Nakamura, J. J. Chalmers
Department of Chemical Engineering, Ohio State University
140 W 19th Avenue, Columbus, OH 43210, USA

L. C. Lasky
Department of Pathology, Ohio State University
140 W 19th Avenue, Columbus, OH 43210, USA

S. Margel
Department of Chemistry, Bar-Ham University, Israel

M. Zborowski
Department of Biomedical Engineering
The Cleveland Clinic Foundation, 9600 Euclid Avenue
Cleveland, OH, USA

Correspondence to: J. J. Chalmers

This work has been supported by the National Science Foundation (BCS9258004, BES-9731059), the National Cancer Institute (R01 CA62349, 1R33 CA81662-01), the US–Israel Binational Science Foundation (96-00486), and the Whitaker Foundation.

Greek symbols

χ	volumetric susceptibility
η	viscosity
μ_0	magnetic permeability of free space
ρ	density

1

Introduction

Analysis and separation of particles or biological cells in a heterogeneous population based on cellular characteristics has applications ranging from fundamental biological studies to clinical practice. These characteristics can include cell density, cell size, and the presence of specific surface markers or molecules on either the surface or within the cell.

With respect to cell size analysis, a number of different cellular attributes have been used to calculate cell size. These attributes are differences in physical size, density, electrical conductivity, and forward angle light scattering (FALS). Examples of commercial units which use several of these attributes are Coulter counters, which use electrical conductivity differences, and fluorescence activated cell scanners/sorters (FACS) which use FALS.

For analysis and separation based on the presence of specific cell surface markers (receptors), FACS are generally used (Shapiro 1995). A typical example is the labeling of cells with antibodies conjugated to a fluorescent molecule(s) such as fluorescein isothiocyanate (FITC).

Analysis and separation of biological cells can also be accomplished through the use of immunomagnetic labels (Moore et al. 1998; Sun et al. 1998; Chalmers et al. 1999a, c). Typically, this labeling is performed using antibodies covalently linked to a paramagnetic carrier. The size of paramagnetic carriers can range from particles (micron size) to paramagnetic colloids (20–200 nm). Commercial examples of both antibodies linked to particles and colloids are available (Miltenyi Biotec GmbH, Bergisch Gladbach, Germany; Immunicon Corp., Huntingdon Valley, Pa.; Dynal Inc., Lake Success, N.Y.).

Actual separations of immunomagnetically labeled cells can be accomplished on relatively simple, commercially available, batch magnetic columns (Miltenyi Biotec GmbH, Bergisch Gladbach, Germany; Immunicon Corp., Pa.) or more advanced flow through systems (Sun et al. 1998; Moore et al. 1998). While batch magnetic columns typically separate cells into “binary mixtures” (cells with and without the paramagnetic label bound), flow systems have the potential to separate cells based on the degree to which the cells are immunomagnetically labeled. However, this more specific separation requires knowledge of the degree to which the cells are labeled. This need for quantification of immunomagnetic labeling led to the current development of an analytical instrument which allows the degree to which a cell is immunomagnetically labeled to be quantified on a cell-by-cell basis. This analytical instrument has been called cell tracking velocimetry (CTV) (Chalmers et al. 1999a–c).

CTV consists of several key components: (1) a well-characterized magnetic field energy gradient; (2) a microscopic image acquisition system; and (3) a computer algorithm derived from a computer algorithm, particle tracking velocimetry (PTV), which can determine the location and velocity of each cell or particle in the region of image analysis. In a previous publication (Chalmers et al. 1999b), the potential of the CTV technique to measure the hydrodynamic diameter of a cell through determination of settling velocities was also discussed.

In this paper, recent improvements in the CTV technique are presented. Specifically, theoretical relationships are developed which indicate the range and limits of the CTV algorithm to measure hydrodynamic diameters and magnetophoretic mobility as a function of video framing rate. These theoretical relationships are then evaluated with size and paramagnetic calibration beads.

2

Relationships governing the movement of particles and cells in the CTV apparatus

The fundamental forces acting on a paramagnetic particle (or immunomagnetically labeled cell) suspended in an aqueous solution are: magnetism, buoyancy, gravity, and drag; expressed as F_m , F_b , F_g and F_d , respectively (Fig. 1). The bold type denotes a vector quantity. When the Reynolds number is less than 0.1, one can assume that F_d is

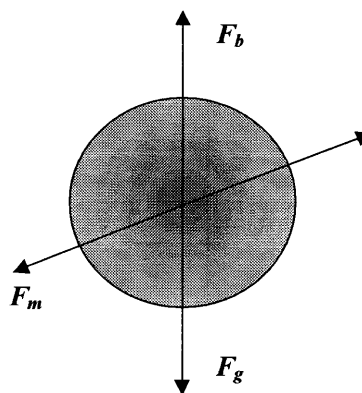


Fig. 1. Schematic illustration of forces acting on paramagnetic particles in solution

represented by the Stokes drag. The magnitude of these forces are defined mathematically as follows:

$$F_m = \Delta\chi V_p \left| \nabla \left(\frac{B^2}{2\mu_0} \right) \right| \quad (1)$$

$$F_g - F_{bou} = \frac{(\rho_p - \rho_f) \pi D_p^3 g}{6} \quad (2)$$

$$F_d = 3\pi v_p D_p \eta \quad (3)$$

where μ_0 is magnetic permeability of free space, $\Delta\chi$ is the difference in volumetric susceptibility between a particle and a fluid, V_p is the particle volume, B is the magnitude of the magnetic flux density, ρ_p is the density of the particle, ρ_f is the density of the fluid, D_p is the particle diameter, g is gravity, v_p is the velocity of the particle, η is the viscosity of the fluid, and ∇ is the nabla operator which produces a gradient when operating on a scalar. The quantity $B^2/2\mu_0$ is a measure of the local magnetic energy density.

In the latest version of the CTV system, the magnetic energy gradient vector was designed to be substantially constant in magnitude, with a primary direction perpendicular to gravity and a small magnitude in the direction of gravity (Chalmers et al. 1999a). In a previous publication, it was shown that all forces balance (Reddy et al. 1996). Consequently, the following relationships can be obtained:

$$u = \frac{\Delta\chi D_p^2}{18\eta} \left| \nabla \left(\frac{B^2}{2\mu_0} \right) \right| \quad (4)$$

$$v = \frac{(\rho_p - \rho) D_p^2 g}{18\eta} \quad (5)$$

where straight brackets denote the magnitude of a vector. In these and all other relationships in this paper, u is the velocity in the direction of the magnetic force, and v is the velocity in the direction of the force due to gravity. In these relationships, it was also assumed that there is no magnetic force in the y direction. However, as will be discussed below, a small, non-zero magnetic force was observed with particles that are paramagnetic. The u velocity is typically “normalized” with respect to the magnetic energy gradient to obtain a magnetophoretic mobility:

$$m = \frac{u}{\left| \nabla \left(\frac{B^2}{2\mu_0} \right) \right|} \quad (6)$$

3 Theoretical performance of CTV

The CTV algorithm is a modification of a 3-D version called particle tracking velocimetry (PTV) (Guezennec et al. 1994). Fundamentally, the original PTV code was optimized to use five successive images to establish the most probable path of a specific particle. From this most probable path, the algorithm determines and reports the 2-D location and velocity for the specific particle in the 3rd (middle) image. This analysis has been theoretically shown to be able to track up to 1,000 particles at a time, although in practice approximately one hundred cells at a time is more common. However, the original PTV algorithm does not report specific cells (particles) tracked from frame to frame, since the algorithm was developed for 3-D flow visualization studies of complex hydrodynamic flow in which the instantaneous velocities of hundreds of locations were desired. Consequently, for this application, the algorithm was modified to provide reports in which the location and velocities of specific cells (particles) are presented for a given series of frames. For example, when a cell is tracked in 20 successive frames, one obtains a report of 16 velocities and locations from each set of five frames (frames 1-5, 2-6, ..., 16-20) and an averaged velocity for the entire data set. This modification allows analysis of the accuracy of the magnetic energy gradient and prevents "multiple" counting of a specific cell (particle) for histogram creation.

A significant limitation of the CTV algorithm is that five consecutive images of a particle must be tracked in order to obtain velocity information. A second limitation involves the reduction of the microscopic image into a digital image. This reduction process, needed for CTV algorithm, is limited by the number, and corresponding "real world" size of a "pixel". Mathematical representations and experimental verification of these limitations constitutes the focus of this paper.

When velocity and/or location information on small particles (~10 microns), such as cells, is desired, magnification is typically needed. In addition, typical video systems, such as the one used in the current apparatus, have a limited field of view and image acquisition rate. The current video system being used produces a visual and digitizable field of view of 1.66 mm by 1.23 mm at a rate of 30 images per second. Since for the current application a video system is used in which each image is referred to as a "frame", for the remainder of this paper the word "frame" will be used for a digitized image. Figure 2 provides a diagram of the field of view. When these magnified images are recorded using a computer, they are recorded in a 2-D matrix of 640 × 480 "pixels". This corresponds to each pixel representing a "real world" location of 2.59 × 2.57 microns. Consequently, depending on the quality of the original image, a 10-micron particle will approximately appear in 12-16 pixels.

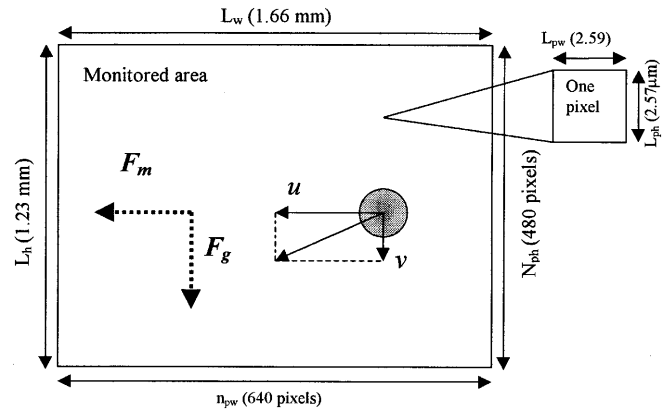


Fig. 2. Diagram of the monitored area in the CTV system including overall and pixel dimensions and the direction of magnetic energy gradient and gravity

3.1 Maximum detectable velocity

Given the previously defined conditions, the maximum, detectable horizontal particle velocity (in the direction of magnetic force) corresponds to the case where the center of a particle appears on the right-hand side edge of a frame, travels across multiple frames, then reaches the left-hand side edge of the fifth consecutive frame (Fig. 3). If the particle moved faster, it would appear in fewer frames; consequently, the CTV algorithm would be unable to report location and velocity data. The same logic applies in the direction in which the force of gravity acts. Mathematically, the maximum velocity of a particle in the direction of the magnetic force, u_{max} , is expressed as follows:

$$u_{max} = \frac{L_w}{(n_c - 1)t_f} = \frac{n_{pw}L_{pw}}{(n_c - 1)t_f} \quad (7)$$

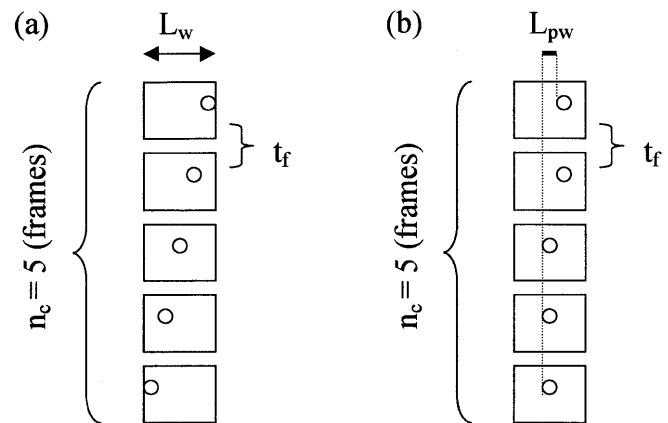


Fig. 3a, b. Diagrams of a sequence of frames demonstrating the movement of a single cell or particle in the direction of magnetic energy gradient (from right to left): a demonstrates the theoretical maximum velocity detectable (cell moves from left to right in five frames); b demonstrates the theoretical minimum velocity detectable (center of cell moves 1 pixel)

where L_w is width of a frame, n_c is the number of frames needed to obtain CTV data (current $n_c = 5$), t_f is the time interval between successive frames, n_{pw} is the number of pixels in width, w , or height, h , of a frame, and L_{pw} is the width and height of a specific pixel. An identical equation can be written for the maximum velocity in the direction of gravity, v_{max} ; however, in this case the constant, L_{ph} , has a slightly different value, since pixels are not square and the value of n_{ph} , which replaces n_{pw} has a value of 480 vs 640.

3.2 Minimum detectable velocity

Though the theoretical minimum velocity that a particle can have is zero, with respect to the CTV apparatus, the theoretical minimum velocity is a function of the magnification and time between successive frames that a specific particle is analyzed. With respect to the separation of an immunomagnetically labeled cell (or particle) in a quadrupole separator, it has been shown recently that several measures of the theoretical performance of the separator is related to the difference in the mean and distribution of the magnetophoretic mobility of the positively and negatively labeled cells (Williams et al. 1999). Consequently, it is desirable to be able to detect low, non-zero values of magnetophoretic mobility. Theoretically, the lowest, non-zero velocity that the CTV apparatus can detect is a velocity in which the center of a particle moved a distance of 1 pixel over five sequential frames. Mathematically, this can be expressed in the magnetic force direction, u_{min} , as:

$$u_{min} = \frac{L_{pw}}{(n_c - 1)t_f} \quad (8)$$

As with the maximum velocity in the direction of gravity, v_{max} , an identical relationship for the minimum velocity in the direction of gravity, v_{min} , can be written, with L_{pw} replaced by L_{ph} .

3.3 Model predictions

There are two primary applications for which the CTV apparatus is being developed: the determination of the hydrodynamic diameter of cells and particles through experimental determination of settling velocities, and the determination of the magnetophoretic mobility of immunomagnetically labeled cells through experimental determination of magnetically induced velocities. Previous studies indicate that the range of settling velocities that will be encountered are approximately 2×10^{-4} to 2×10^{-2} mm/s, and for magnetically induced velocities this range is 1×10^{-5} to 1×10^{-1} mm/s. Given these ranges of v and u , the number of pixels which define the field of view, the dimensions of an individual pixel and the above relationships [Eqs. (7) and (8)], one can calculate the time interval between successive frames, t_f , needed to be able to detect a given velocity. Figure 4 is a plot of minimum and maximum settling and magnetic velocity as a function of t_f using the above information at Eqs. (7) and (8).

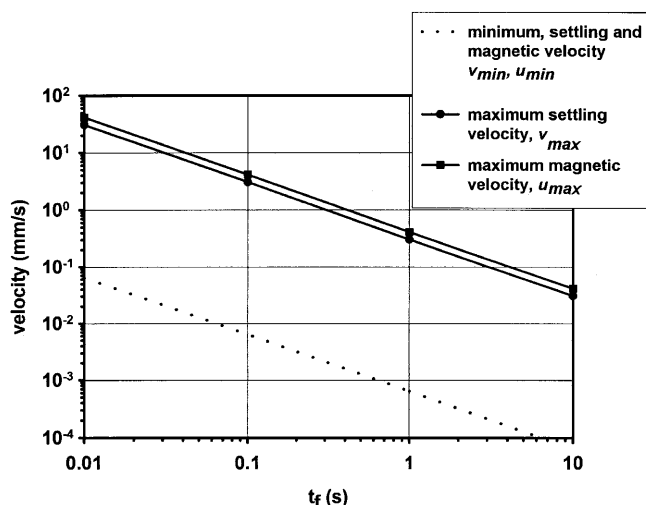


Fig. 4. Graphical representations of the model predications for the range of performance of CTV for settling velocity and magnetically induced velocity. Note that the minimum settling velocity and magnetic velocity are virtually the same, hence only one line is presented

4 Materials and methods

4.1 Experimental apparatus

The currently used experimental apparatus, with minor modifications, has been reported previously and will only briefly be summarized here (Chalmers et al. 1999a). A suspension of cells or particles to be analyzed is pumped into a square borosilicate glass channel (1.0 mm I.D., 1.4 mm O.D.) which is mounted within a specifically defined magnetic energy gradient, $\nabla B^2/2\mu_0$. An Olympus BHMJ microscope using a 5 \times objective and 2.5 \times photoeyepiece was used to record the movement of these cells or particles in a specific location in which the magnitude of $\nabla B^2/2\mu_0$ is nearly constant. A 150-W halogen lamp fiber optic cable system (Fiber Lite, Dolan Jenner, Lawrence, Mass.) was used to supply light through the microscope. (This microscope has an internal lighting option.) A CoHU CCD 4915 camera (San Diego, Calif.), which has an active picture element resolution of 768(horizontal) \times 494(vertical) and a framing speed of 30 Hz was used. A Sony SVO-9500MD S-VHS video recorder was used to record particle movement. Recent improvements in the system include the addition of a two-way syringe pump (PhD 2000, Harvard, Mass.), which is computer controlled. This allows more precise delivery of the flow of cell or particle suspensions of interest.

4.2 Computer imaging and CTV algorithms

As with the experimental apparatus, the process of observing, computer imaging, and determination of the particle or cell location and velocity has been previously reported (Chalmers et al. 1999a-c). However, in contrast to previous studies, an improved image grabbing board was used in this study: μ m-Tech Vision 1000 PCI

(μ -Tech Corp, USA). This new image grabbing board is a significant improvement over previous boards used and reported. Specifically, it allows the operator to choose the time interval between successive frames (up to the limit of the camera which was 30 frames/s) and has improved gain and offset adjustments. This new board improved the quality of the images to such an extent that all of the previously reported post image grabbing processing steps are not needed, except image subtraction, for the particles used in the current study. In conjunction with this new μ -Tech image grabbing board, a program was written which allows the user to select the region of interest to digitize. The introduction of this feature reduced the noise in digitized images. Finally, the μ -Tech board operates in a Windows 95 environment.

These digitized images were then processed using the CTV algorithm. The CTV algorithm defines a contiguous set of pixels that exceed a minimum level of contrast with the background image as an object. User-defined requirements for cell size (minimum and maximum number of pixels per object) and shape (length to width ratio of object) are then used to determine whether the object will be considered a cell (particle). Each cell is identified and labeled by the CTV algorithm based on its size, shape, and location of its center.

4.3 Calibration particles

Two type of particles were used in this study: polystyrene size calibration particles from Duke Scientific (Palo Alto, Calif.), and paramagnetic particles from the laboratory of Dr. Shlomo Margel, of Department of Chemistry, Bar-Ilan University, Ramat Gan, Israel. Three sizes of polystyrene beads were used: 7.0, 9.0, and 14.1 microns, with coefficients of variation of 5.7, 10.0, and 8.5, respectively. These beads have a density of 1.05 g/ml. A more complete discussion of the paramagnetic particles can be found in Moore et al. (2000).

5 Results and discussion

5.1 The effect of t_f on settling velocity measurements

The model predictions presented in Fig. 4 indicate that there is a maximum and minimum detectable particle velocity for a specific t_f value using the CTV algorithm. In practice, in addition to this theoretical limitations incorporated into the model, there are practical, experimental limitations as well. One of these major limitations is identification of the particle "size" from frame to frame. This can be especially difficult for cells that do not have as high a contrast with respect to the background as do solid particles. However, even with solid particles changes in "size" can result from differences in light in different fields of view and the particles moving into or out of the thin plane of focus of the objective (approximately 16 microns for a 5 \times). This change in "size" from frame to frame can result in the particle "jumping", or having large changes in velocity from frame to frame.

Figure 5 presents histograms of the settling velocity of three sizes of Duke beads (7.0, 9.0, and 14.1 microns; a, b, c, respectively) using four different values of t_f : 0.033, 0.167, 0.667 and 2 s. These results are also reported in Table 1 along with the size of the population, mean and coefficient of variation, CV. The size of the population refers to the number of distinct particles (beads) that were tracked.

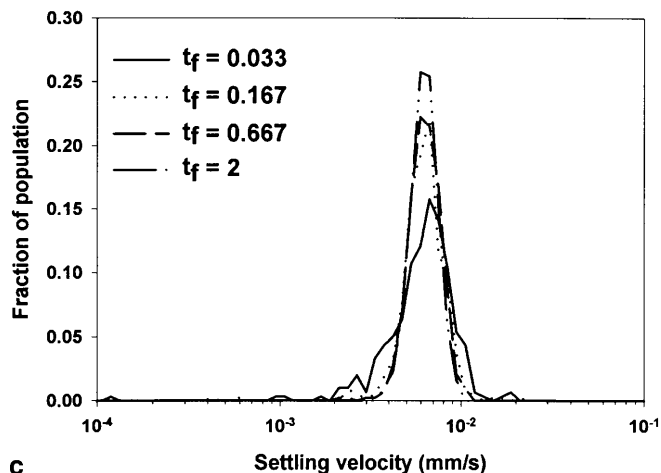
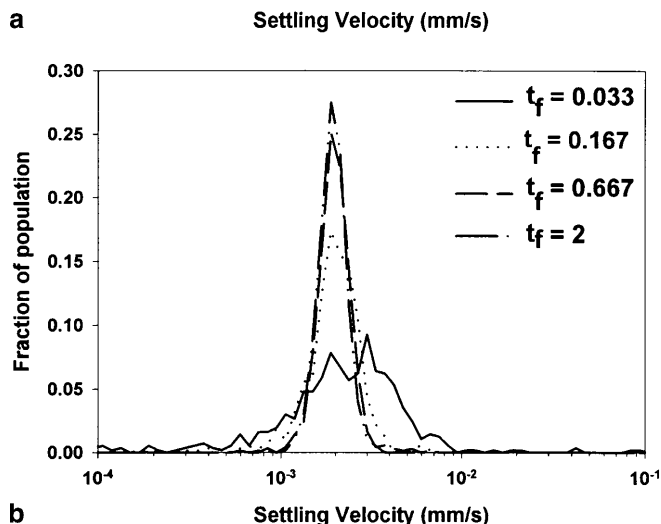
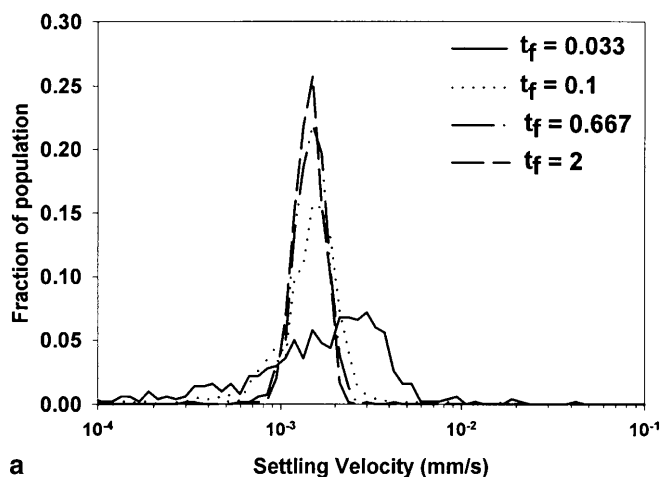


Fig. 5a-c. Effect of time interval (t_f) on settling velocity distribution of respective Duke beads: a #1; b #2; c #3

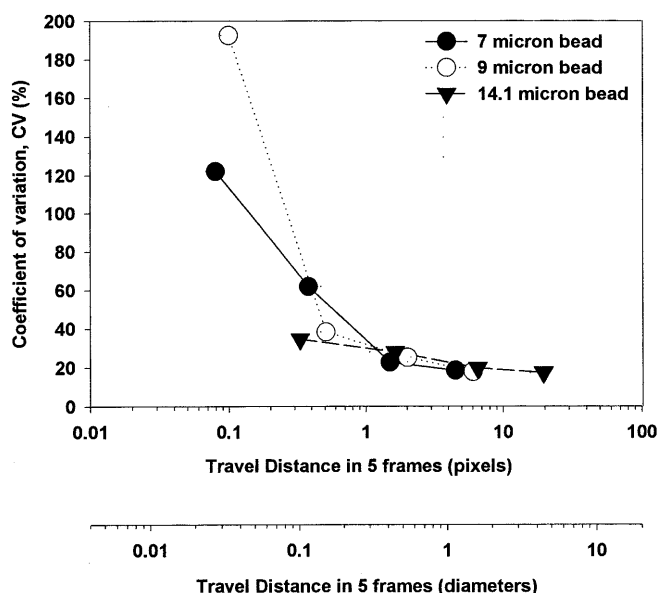
Table 1. Effect of t_f (time between frames) on measured settling velocity of Duke beads

Bead diameter [μm]	t_f [s]	N [beads]	Mean $\times 10^3$ [mm/s]	CV
7.0	0.033 (1/30)	500	2.26	122.1
	0.167	683	1.58	62.0
	0.667	671	1.49	22.8
	2	614	1.45	18.6
9.0	0.033	562	3.12	192.6
	0.167	634	2.06	38.3
	0.667	713	2.02	25.2
	2	596	1.95	17.9
14.1	0.033	298	6.48	34.6
	0.167	426	6.40	28.0
	0.667	423	6.43	19.8
	2	303	6.33	17.4

It is important to note that a specific particle is typically tracked in more than five frames. Consequently, typically more than one location and velocity data set are available for any specific particle. For example, if a particle is tracked in ten sequential frames, six sets of data are obtained. However, during the creation of the histogram (and the mean and CV reported in Table 1), if more than one data set for a specific particle is available, only a single, mean velocity from that data set is used.

The trends in the experimental results were expected. Specifically, Fig. 5a–c and Table 1 demonstrate that the distribution of settling velocity, both qualitatively visible in the “spread” of the histograms and quantitatively through the use of the coefficient of variability, CV (100 times the standard deviation divided by the mean), decreases as t_f increases. Also of interest is the observation that the larger the bead (and, correspondingly, the higher the settling velocity), the less effect the same values of t_f has on the CV over the range studied. The smaller the distribution of a histogram, or CV, the more precise the analysis.

This observation that CV drops with increasing t_f was quantitatively predicted in the model. Specifically, Fig. 4a predicts that for settling velocities of 1.46×10^{-3} mm/s, 1.95×10^{-3} , and 6.3×10^{-3} (the mean settling velocities of Duke Beads #1, #2 and #3), minimum values of t_f of 0.44, 0.33, and 0.101 s, respectively, should be used. These minimum values of t_f are within the range of t_f used in this study. To further understand this effect of t_f , Fig. 6 was created. In this figure, the CVs for Duke beads #1, #2, and #3 were plotted as a function of the travel distance in five frames in units of pixel and bead diameter for each of the experiments reported in Fig. 5a–c and Table 1. The model assumed that the center of the cell or particle had to move 1 pixel distance in five frames to be accurately detected. Consequently, a travel distance of 1 pixel corresponds to the minimum value of t_f which should be used (Fig. 4). Figure 6 indicates that the highest values of CV occur for travel distances less than 1 pixel distance. Also, a clear trend exists, with the largest drop in CV occurring as the value of t_f is increased to approximately 1 pixel. After reaching a travel distance of approximately 1 pixel in five frames, increasing t_f has little effect on CV.

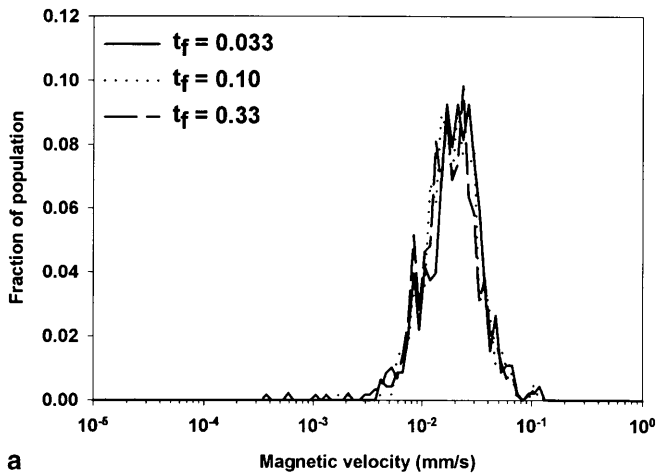
**Fig. 6.** The relation between the coefficient of variation of settling velocity of Duke beads and the travel distance in five frames in units of pixels and bead diameters

High variations, as indicated by a high value of CV, for velocity distributions measured at t_f values lower than the minimum t_f calculated by the model could be explained by experimental error in determining the displacement of the particle center. At low values of t_f , average particle displacement becomes very small (0 or 1 pixel per five frames). Errors in tracking may result from the measurement of very small particle displacements attributable to changes in focus of the particle or the reflection of light, rather than actual particle movement.

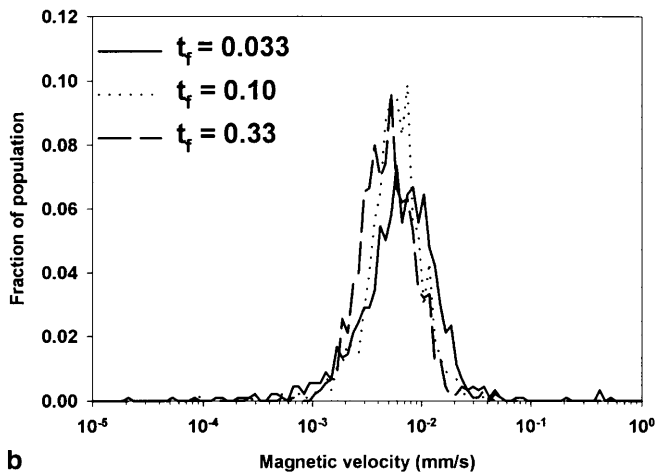
5.2 The effect of t_f on magnetically induced velocity measurements

A study on the effect of t_f on the distribution of the magnetically induced velocity, which was similar to the study on the settling velocity with the Duke beads, was also conducted. A total of five populations of the paramagnetic beads were evaluated. Two of the bead populations have a sufficiently high level of magnetophoretic mobility (velocity) that those populations were only evaluated with the highest number of frames per second currently possible, t_f equal to 0.033. The other three populations were evaluated at three different values (four different values for population number 5) of t_f and the results are presented in Fig. 7a–c and Table 2. The actual magnetic characteristics of these beads were described in detail in a previous publication (Moore et al. 2000).

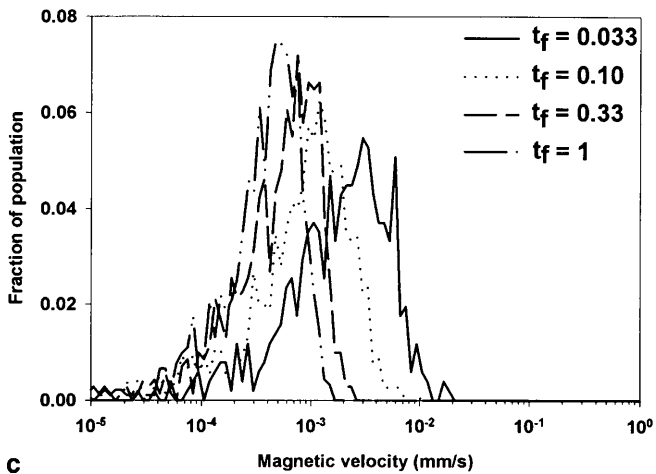
Similar observations and analysis can be performed for the magnetically induced velocities as was done with the settling velocity studies. For these studies with the magnetic beads, the model predicts that the minimum values of t_f are approximately 0.03, 0.092, and 1.35 s for the populations of magnetic beads numbered 3, 4, and 5, respectively. As can be observed in Fig. 7a and Table 2, this minimum value of t_f , 0.03, was the lowest value of t_f at



a



b



c

Fig. 7a–c. Effect of time interval (t_f) on magnetic velocity distribution of magnetic beads: a #3; b #4; c #5

which the system can be experimentally operated. Consistent with that fact, the CV of the experiments on the third population of magnetic beads did not noticeably change with increasing t_f . While the predicted minimum value of t_f for the fourth population of magnetic beads was slightly higher than the minimum value at which the system can operate, again no noticeable change in CV was observed with increasing values of t_f . Only with magnetic

Table 2. Effect of t_f on measured magnetic velocity of the magnetic beads

Beads	t_f [s]	N [beads]	Mean $\times 10^3$ [mm/s]	CV [%]
M#3	0.033	454	23.0	62.8
	0.10	604	21.6	63.2
	0.10 ^a	1,250	23.6	53.5
	0.33	580	21.0	65.8
M#4	0.033	834	7.76	85.1
	0.10	880	6.81	82.3
	0.33	902	6.08	88.5
M#5	0.033	512	2.71	90.3
	0.10	753	1.23	85.3
	0.33	709	0.65	66.1
	1	916	0.46	61.4

^a Indicates an experiment conducted four months after the experiment which produced the data in the previous row

bead population number 5 were significant changes in histogram distribution and CV values observed (Fig. 7c and Table 2).

As with the settling velocity studies, plots of CV vs travel distance in five frames were also constructed and presented in Fig. 8. Also, as with the settling velocity studies, the CV drops with increasing travel distance until that distance approaches 1 pixel. However, as can be observed in both Fig. 8 and Table 2, the CV, even after optimization of t_f , is still quite high when compared with that of the Duke Scientific beads. The high value of CV is most likely the result of a relatively wide distribution in magnetic material loading rather than an analytical error. However, we cannot confirm this hypothesis, since we know of no other analytical instrument that can measure the magnetically induced velocity on a particle-by-particle basis.

5.3

Reproducibility of velocity measurements

To test the reproducibility of the system, the settling velocities of each of the three Duke bead populations were measured on three consecutive days with a t_f value of 2 s for each bead size. As with previous experiments, these data are presented in the form of a histogram in Fig. 9 and in tabulated form in Table 3.

To test the statistical significance of these repeated studies, a non-parametric, Kruskal–Wallis one-way analysis of variance on ranks was conducted using the computer software SigmaStat (Jandel Corporation, San Rafael, Calif.). Specifically, the three repeated studies of each Duke bead population were pairwise tested. The results of the analysis indicated that there is no statistical difference ($P < 0.001$) between the three studies conducted on the 14.1-micron Duke beads. However, with both the 7.0- and 9.0-micron Duke beads, this analysis indicated that there is a statistical differences between several pairs. It can be observed in Table 3 that the differences in the mean values are quite small; yet this analysis indicates that the differences are significant. At this stage we do not know the cause of this variation.

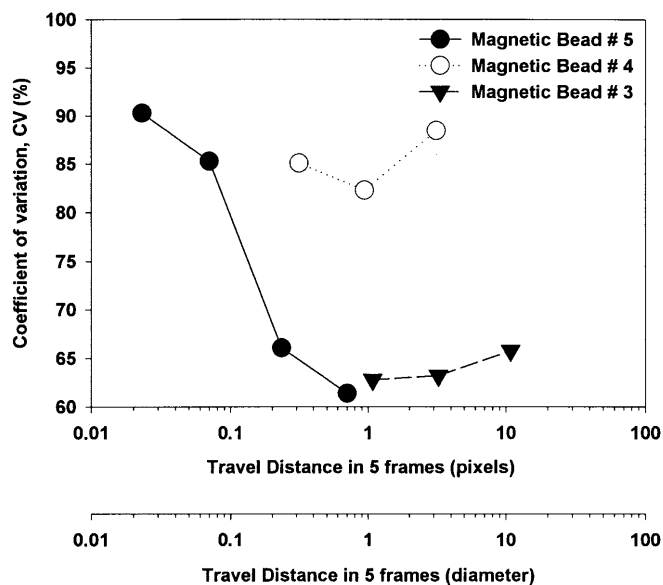


Fig. 8. The relation between the coefficient of variation of magnetically induced velocity of magnetic beads and the travel distance in five frames in units of pixels and bead diameters

Figure 10 presents two histograms of the CTV-calculated magnetically induced velocities of magnetic bead number three. The interval of time between these two experiments was four months. As with the repeated settling velocity measurements, a non-parametric, Kruskal-Wallis one way analysis of variance on ranks test was conducted on the two data sets. As with two of the three sizes of Duke beads, the test indicated that there is a statistical difference between the two experiments. Table 3 indicates the difference in mean velocity between these two experiments was 8.5%. At this time, the reason for this difference is unknown.

5.4

Comparisons of Duke bead diameters

A further test of the accuracy of the CTV technique is to compare the diameter calculated from the experimentally determined settling velocity with the information provided by Duke Scientific Corp. and the experimental data from a Coulter counter. To obtain diameters from settling velocity data, the following relationship was used:

$$D_p = \left[\frac{18\eta v}{g(\rho_p - \rho)} \right]^{\frac{1}{2}} \quad (9)$$

where D_p is the particle diameter, ρ_p is the manufacturer's provided density of the particles, and v is the CTV determined settling velocity. Figure 11 presents histograms which compare the sizes of the three populations of Duke beads between the manufacturer's specifications, the Coulter counter results and the calculated diameters using Eq. (9), and the mean of the experimentally determined settling velocities. The mean and CV from the manufacturer, the CTV, and the Coulter counter studies are also presented in Table 3. While some variation exists when the manufacturer's specifications are compared with the CTV

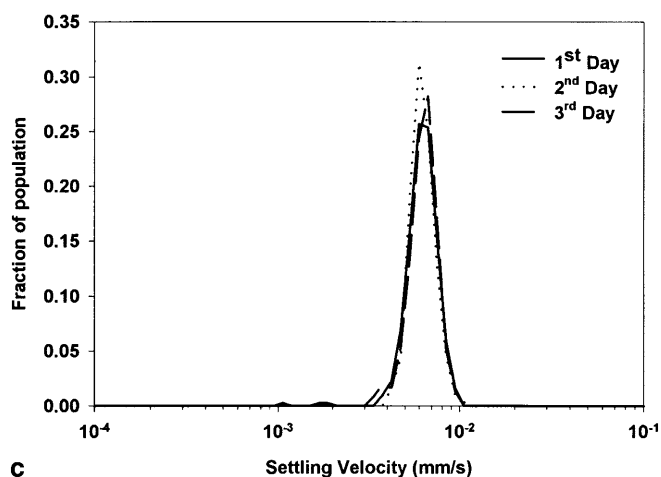
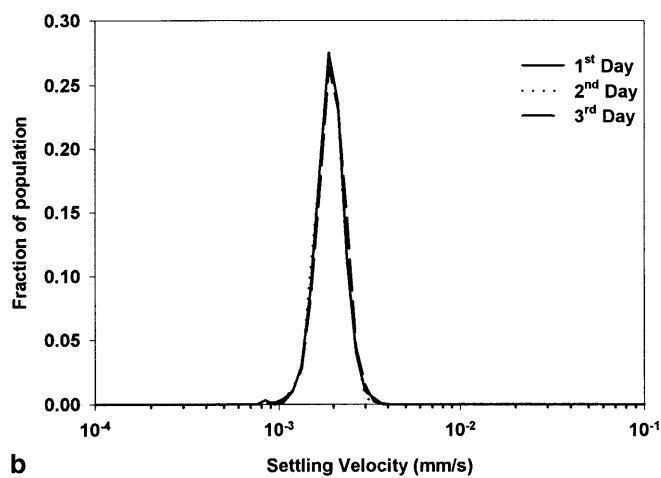
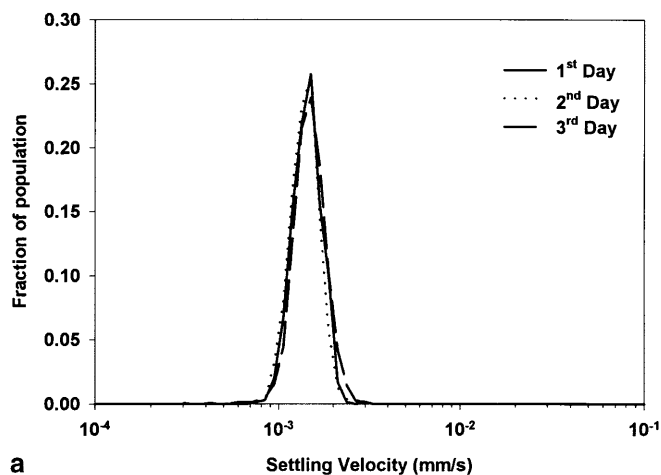


Fig. 9a-c. Repeatability over a period of days of settling velocity measurement in CTV: a Duke bead #1; b Duke bead #2; c Duke bead #3

and Coulter counter data, in general the agreement is reasonable. Why the CTV technique over-predicted the particle diameter in two cases is currently under investigation.

5.5

Magnetophoretic mobility distributions

The last histogram, Fig. 12, is a composite of the distribution of the magnetically induced velocity, or the

Table 3. Measured settling velocity (SV) and calculated hydrodynamic diameter (HD) by CTV and diameter by Coulter counter

Manufacturer's specifications		CTV				Coulter counter			
[μm]	CV [%]	N	$\text{SV} \times 10^3$ [mm/s]		Calculated HD [μm]		N	Diameter [μm]	
			Mean	CV [%]	Mean	CV [%]		Mean	CV [%]
7.0	5.7	641	1.45	18.3	7.34	9.13	3,912	7.16	6.70
		1,505	1.41	18.6	7.24	9.17	4,039	7.18	7.71
		1,171	1.51	19.8	7.47	9.91	4,186	7.14	6.89
Avg			1.46	18.9	7.35	9.41		7.16	7.11
9.0	10	596	1.95	17.9	8.51	8.99	866	9.07	9.01
		1,200	1.92	17.2	8.45	8.67	839	9.12	8.24
		1,386	1.97	18.2	8.56	9.14	833	9.03	10.26
Avg			1.95	17.8	8.51	8.93		9.07	9.16
14.1	8.5	303	6.33	17.4	15.3	8.74	2,042	13.99	8.43
		300	6.31	15.5	15.3	7.57	2,003	13.98	8.44
		361	6.30	18.4	15.3	9.88	1,959	13.96	8.24
Avg			6.31	17.1	15.3	8.7		13.98	8.37

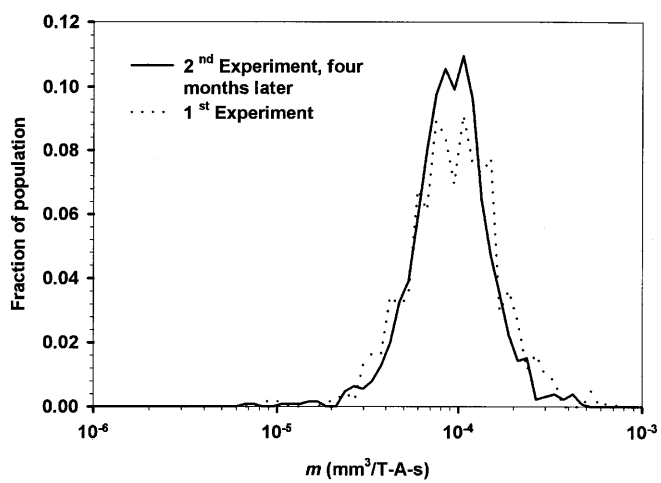


Fig. 10. Repeatability over a period of four months of the magnetically induced velocity of magnetic bead population number 3

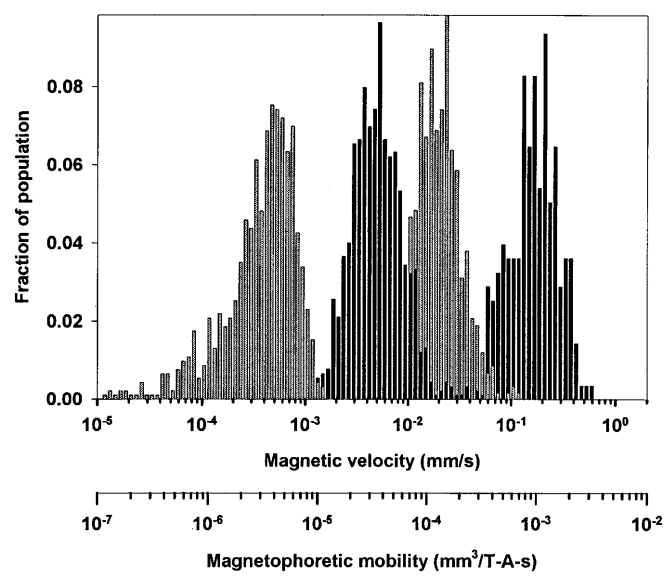


Fig. 12. Magnetophoretic mobility distributions of magnetic beads numbers 2-5

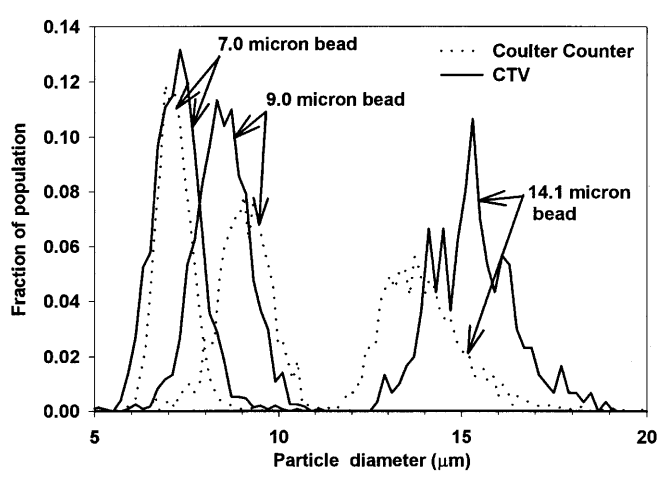


Fig. 11. Settling velocity and hydrodynamic diameter of Duke beads obtained by CTV and diameter of Duke beads measured by Coulter counter

magnetophoretic mobility, of the five paramagnetic bead populations using the appropriate model predictions for values of t_f . The magnetophoretic mobility was calculated by dividing the magnetically induced velocity by 198 T A/mm^2 , the magnitude of magnetic energy gradient, $\nabla B^2/2\mu$.

6

Conclusions

The above model, experimental results and discussions indicate that the appropriate choice of time interval between frames, t_f , can have a significant effect on both the mean and distribution of experimentally determined velocities using the CTV system. These effects are most pronounced at low velocities. Also, the close agreement of the reported characteristics of the Duke calibration beads with both the CTV and Coulter counter lends further

evidence to the validity of the CTV technique to characterize the size of micron-size particles.

An additional observation is the reproducibility of the system. This reproducibility is partially the result of the relatively simple experimental measurement: cell (particle) velocity. This measurement does not require a special resuspending buffer of specific ionic characteristics (as does the Coulter counter), nor calculations of the deflection of laser beams. This lack of need for specific ionic buffers can be particularly important with biological samples. Once properly assembled, and if needed, corrected for any lens distortions, the system is potentially indefinitely stable. The use of permanent magnets also contributes to the stability of magnetically induced velocity measurements. This is in contrast to a similar instrument, FACS, which requires daily calibration.

References

- Chalmers JJ; Zhao Y; Nakamura M; Melnik K; Lasky L; Moore L; Zborowski M (1999a) An instrument to determine the magnetophoretic mobility of paramagnetic particles and labeled, biological cells. *J Magn Magn Mater* 194: 231–241
- Chalmers JJ; Haam S; Zhao Y; McCloskey K; Moore L; Zborowski M (1999b) Quantification of cellular properties from external fields and resulting induced velocity: Cellular hydrodynamic diameter. *Biotechnol Bioeng* 64: 509–518
- Chalmers JJ; Haam S; Zhao Y; McCloskey K; Moore L; Zborowski M (1999c) Quantification of cellular properties from external fields and resulting induced velocity: Magnetic susceptibility. *Biotechnol Bioeng* 64: 519–526
- Guezennec YG; Brodkey RS; Trigui N; Kent JC (1994) Algorithms for fully automated three-dimensional particle tracking velocimetry. *Exp Fluids* 17: 209–219
- Moore LR; Zborowski M; Sun L; Chalmers JJ (1998) Lymphocyte fractionation using immunomagnetic colloid and dipole magnet flow cell sorter. *J Biochem Biophys Methods* 37: 11–33
- Moore LR; Zborowski M; Nakamura M; McCloskey K; Gura S; Zuberi M; Margel S; Chalmers JJ (2000) The use of magnetic-doped polymeric microspheres in calibrating cell tracking velocimetry. *J Biochem Biophys Methods* (in press)
- Reddy S; Moore LR; Sun L; Zborowski M; Chalmers JJ (1996) Determination of the magnetic susceptibility of labeled particles by video imaging. *Chem Eng Sci* 51: 947–956
- Shapiro H (1995) *Practical flow cytometry*. John Wiley, New York
- Sun L; Zborowski M; Moore L; Chalmers JJ (1998) Continuous, flow-through immunomagnetic cell sorting in a quadrupole field. *Cytometry* 33: 469–475
- Williams PS; Zborowski M; Chalmers JJ (1999) Flow rate optimization for the quadrupole magnetic cell sorter. *Anal Chem* 71: 3799–3807